The Kinetic Modeling and Computer Simulation of Catalytic Hydrogenation of 2,4-Dinitrotoluene over Platinum Nanoparticles

* Mohammad Reza Saboktakin[1,2], Roya M.Tabatabaie[1], Abel Maharramov[2], Mohammad Ali Ramazanov[2]
1 Nanostructured Materials Synthesis Lab., International Research Institute of Arian Chemie Gostar,Tabriz,Iran
2 Nanotechnology Research Center , Baku State University ,Baku ,Azerbaijan
saboktakin123@yahoo.com

Abstract: Kinetic models are an essential part of modern computer simulation (HYSYS) based on process design.The goal of the work presented here was to develop model for heterogeneous hydrogenation reaction of 2,4-dinitrotoluene using platinium nanoparticles (100 nm) as catalyst .The studied reaction is important in the production of new, environmentally friendly fuels. The hydrogenation was assumed to proceed by a mechanism of stepwise addition of dissociatively adsorbed hydrogen.Langmuir-Hinshelwood type rate equations were able to describe the reaction kinetics successfully, including the inhibition effect.The kinetic equations developed in this work are applicable as such in reactor design because mass transfer, hydrogen solubility were taken into account in the parameter optimization.
[Mohammad Reza Saboktakin, Roya M.Tabatabaie, Abel Maharramov, Mohammad Ali Ramazanov. **The Kinetic Modeling and Computer Simulation of Catalytic Hydrogenation of 2,4-Dinitrotoluene over Platinum Nanoparticles**. Researcher. 2011;3(1):1-8]. (ISSN: 1553-9865). http://www.sciencepub.net.

Keywords: kinetic modeling, computer simulation, hydrogenation ,2,4-dinitrotoluene, platinium , nanoparticles.

1. Introduction

The increased attention paid to catalytic hydrogenation in the oil refining industry is due in part to legislation regarding the maximum contents of sulfur,aromatic compounds ,and alkenes in traffic fuels (Nishimura, S., 2001- Kabalka, G. W.; Vama,R.S., 1991) [1,2] . Key objectives in the development of new hydrogenation processes include the development of more active catalysts as well as accurate kinetic models that based on reaction mechanisms (Rylander, P., 1979- Tundo, P., 1991) [3,4]. When carried out on the industrial scale, the reactions related with this work are performed in the liquid phase,in order to avoid excessive energy consumption during the vaporization of the reactants (Ehrfeld, W.; Hessel, V.; Lowe, H., 2000- Zhang,L.; Rana, T., 2004) [5,6]. Using the liquid phase complicates kinetic studies and makes most of the in –situ techniques for mechanistic determinations impossible.Higher concentrations and equilibrium limitation in the hydrogen solubility in the liquid phase may, however,substantially change the hydrogenation and deactivation rates (Tri, T.M.; Massadier, P.; Gallezot, P.; Imelik, B., 1982- Moreau, C.; Geneste, P., 1990) [7,8]. With this in mind,it appeared prudent to perform the experiments under conditions as close to the industrial operating conditions as possible, that is the liquid phase at moderate temperatures and elevated pressures (West, A.R., 1998- Klug, H.P.; Alexander, L.E., 1954) [9,10]. The original part of the present study concerned the hydrogenation of 2,4-dinitrotoluene (Fukai,Y., 1993)[11] .Kinetic models were developed that can be used in the design and optimization of industrial-scale reactors.Rate equations (generalized Langmuir-Hinshelwood type) were based on the assumption of a stepwise adition mechanism of adsorbed hydrogen atoms (Winter, C.J.; Nitsch, J., 1988) [12] .Kinetic parameters were optimized from the data obtained on a Pt/C nanoparticles as catalyst. Also, we have caculated kinetic parameters by computer simulation (HYSYS). The experimental data have shown good compatibility with computer simulation data (Cox, K.E.; Thompson, A.W.; Bernstein,I.M.,1976- Allen, L.; Suchanek, A., 1998) [13,14].

2. Experimental Part

2.1 Test Reactor

Hydrogenation experiments were performed in a continuous strirred laboratory-scale three-phase reactor equipped with a fixed catalyst basket and a magnetic stirrer. The gas (258 cm^3) and liquid (50 g/h) feeds were regulated using mass flow controllers. The reaction pressure was maintained at the desired level by regulating the gas outlet stream,which was separated from the liquid product in a high-pressure separation unit.The liquid product samples were analyzed on-lined using a gas chromatograph with a fused silica capillary column and FI detector.Figure 1 shows the reactor model applied in the estimation of kinetic parameters.

2.2 Mass –Transfer Experiments

The gas – liquid and liquid-solid mass – transfer resistances were determined experimentally

by varying the catalyst loading in the reactor.An estimate of the external mass-transfer limitations could be made by plotting the reciprocal of the conversion rate(mol/h) as a function of the reciprocal of catalyst mass and extrapolating the catalyst mass to a an infinitely high value(intercept with the $1/m_{cat}$ axis).The mass-transfer rates thereby obtained were considerably higher than the maximum reaction rates observed in the kinetic experiments.Thus ,it was concluded that external mass transfer did not have an effect on the observed rates in the hydrogenation experiments.Experiments with nanoparticles and high values of the weisz-prater.However,that internal mass-transfer limitations could not be avoided with the available experimental setup.The size of screen opening in the catalyst basket meant that only particles about nanometer could be used.Therefore, in the optimization of kinetic parameters, a model for the diffusion resistance inside the catalyst particles had to be included in the reactor model.

2.3 Kinetic Experiments

Each experiment was carried out with fresh catalyst that had first been dried at 110°C in N_2 . Prior to starting the liquid feed, the catalyst was reduced in situ at 400°C for 2 hours with mixing in flowing hydrogen. Experiments in the continuously operating reactor were typically divided into periods of 4-5 h with different reaction conditions (temperature, pressure, and feed concentrations) (Tables 1,2). In addition,a standard period with reference conditions was included at the beginning and end of the experiment to monitor the catalyst activity.This arrangement enabled collection of extensive data sets and elimination of the effect of catalyst deactivation on observed hydrogenation rates.In this work , the pressure range was 20-40 bar, and temperatures of 85-160°C were used.

3. Kinetic Modeling

3.1 Models for mass and Heat Transfer

The mass-transfer rate between the gas and liquid phases was described using the two-film theory(1).Since experiments with various catalyst loadings had shown that the external mass transfer did not limit the rates of the reactions ,high values were assigned for the mass-transfer coefficients in the gas and liquid films($\kappa G_\alpha G_L = 1.0 \times 10^4\ s^{-1}$ and $\kappa G_\alpha G_L = 1.0 \times 10^2\ s^{-1}$) (Tables 3,4) .The equilibrium constants at the phase interface (KG_L,i) were evaluated using the Soave-Robinson(PR) equation of state have been experimentally proven to be accurate methods for the calculation of vapor –liquid equilibrium between hydrogen and 2,4-dinitrotoluene.The reason for choosing the PR instead of the SRK equation of state was that it is reported to produce a slightly better fit for mixture of hydrogen with a carbon number less than 20(Table5).

Diffusion inside the porous catalyst particles was described using the effective diffusion coefficients, *D*eff, which account for the mass-transfer restriction due to porous matter in accordance with where *D* is the molecular diffusion coefficient, and εp and τp stand for the porosity and tortuosity inside of the particles, respectively(2). Molecular diffusion coefficients were estimated by the Wilke–Chang method, and the values of εp and τp for the different catalysts were obtained by the literature methods(Tables 6) . The mass-transfer rate between the liquid phase and the porous catalyst (observed reaction rates, *N*LS,*ia*LS) was obtained from the solution of the mole balance for the catalyst nanoparticles(3), where λ stands for the dimensionless position inside the catalyst nanoparticles ($0 \le \lambda \le 1$) and *r*p and ρp for the radius and density of the catalyst particles, respectively (Table 7). Parameter *B* is the shape factor of the catalyst nanoparticles, which is defined by where *A*p and *V*p stand for the outer surface area and volume of the nanoparticles, respectively. Crushed and sieved fractions of the Pt/C catalyst was used, and therefore *B* had a value of 3 (spherical geometry)(4).

The strong deactivation on Pt/C forced the use of nanometer-size particles, which were long, cylindrical in shape and had a *B* parameter value of 2. The partial differential equation 4 was solved by discretizing it with respect to the position inside the particle (λ) using a five-point central difference formula. The mass-transfer rates at the liquid–solid interface (apparent rates), *N*LS,*ia*LS, were then calculated by summing up the rates in each discretization interval(Table 8).

The gas and liquid bulk phases were assumed to be isothermal because the temperature of the stirred reaction vessel was controlled using external heating and cooling (± 0.5 °C). Furthermore, the maximum temperature difference inside the 0.5 mm Pt/C catalyst nanoparticles were less than 0.3 °C(5). Therefore, the heat transfer in the catalyst could be ignored in the kinetic models. Also, because the nanoparticle size was used, isothermal particles could be assumed. For this reason, the dynamic energy balance described by equation (6) was used to describe the temperature profile inside the catalyst nanoparticles (Table 9).

In equation 6, the values of –113 kJ/mol and –117 kJ/mol were used for the heats of reaction (Δ*H*R) in the hydrogenation of 2,4-dinitrotoluene, respectively ,where the calculated volumes were obtained using the Soave–Redlich–Kwong (SRK) or Peng–Robinson(PR) equation of state and

experimental volumes were determined by step response experiments.

The linear system of ordinary differential equations (7) and (8) was integrated numerically using the Flowbat flowsheet simulator.A routine based on the semi-implicit Runge–Kutta method was used . The integrator was developed further in order to minimize the computation time. A hybrid integrator was implemented, which alternated dynamically between two calculation routines: one based on the semi-implicit Runge–Kutta and the other on the Gear and Adams–Moulton method (VODE) (Table 10).

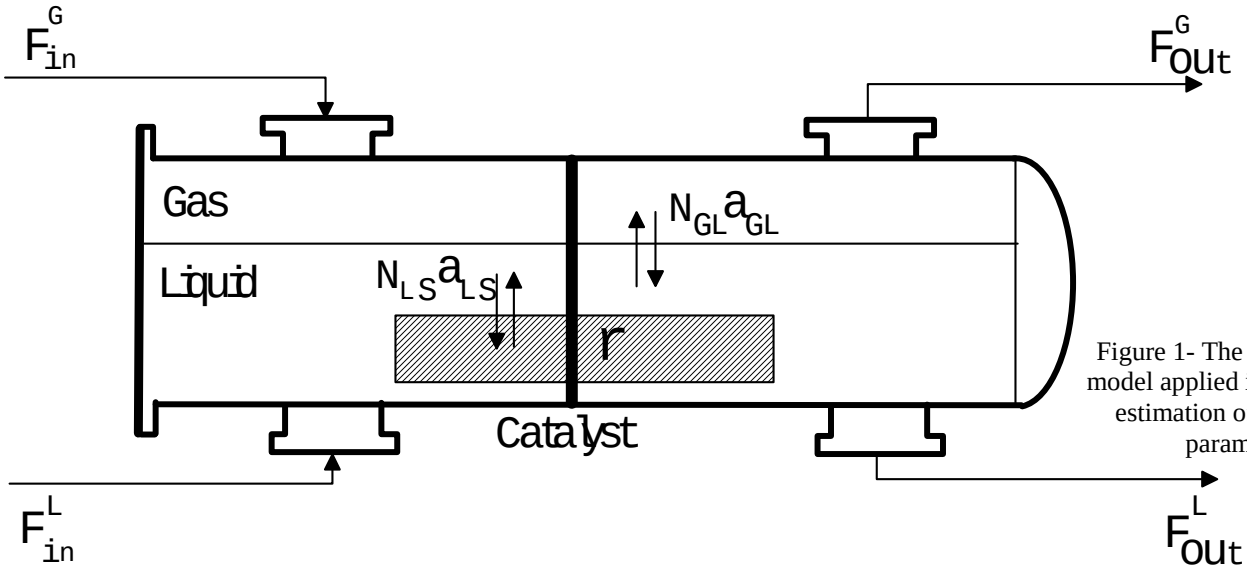

Figure 1- The reactor model applied in the estimation of kinetic parameters

Table 1 – Additional Point Properties

Property Package Molecular Props	
PRSV-Kappa	-0.45523
KD Group Parameter	0.00000
ZJ EOS Parameter	0.00000
GS/CS-Solubility Parameter	11.18045
GS/CS-MOL Vel[m3/kgmole]	0.13399
GS/CS-Acentricity	0.71257
UNIQUAC- R	9.70887
UNIQUAC-Q	8.02696
WilsonMOlar Volume [m3/kgmole]	0.13399
CN Solubility	11.18045
CN Molar Volume [m3/kgmole]	0.13399

Table 2 – Base Properties / Critical Properties

Molecular Weigth	182.14
Normal Boiling Pt[C]	316.85
Ideal Lig Density { kg/m3]	1374.05
Temperature [C]	540.85
Pressure[kPa]	3400.00
Volume[m3/kgmole]	0.48700
Acentricity	0.71257

Table 3 – Temperature dependent Properties

Antoine Vapour Pressure In[P]= a + b/[T+c] + d*ln[T]+e*T^f Pressure,P[kPa] T[K]	
Min Temperature[C]	69.50
Max Temperature[C]	540.85
Coefficient Name	Antoine Coeff.
a	1.38640e+02
b	-1.39900e+0.4
c	0.00000e+01
d	-1.77620e+01
e	8.63450e+06
f	2.00000e+00
g	0.00000e+01
h	0.00000e+01

Table 4- Additional Point Properties

Thermodynamic and Physical Props	
Dipole Moment[Debye]	4.31701
Radius of Gyration[Angstrum]	5.07000
COSTALD[SRK]Acentricity	0.71257
COSTALD Volume[m3/kmole]	0.48700
Viscosity Coeff A	0.44993
Viscosity Coeff B	0.43057
Cavett Heat of Vap Coeff A	0.25364
Cavett Heat of Vap Coeff B	<empty>
Heat of Form[25C][kJ/kmole]	3.320e+004
Heat of Comb[25C][kJ/kmloe]	-3.416e+006
Enthalpy Basis Offset[kJ/kmole]	1.071e+004

Table 5- Temperature Dependent properties

Antoine Vapour Pressure In[P]= a + b/[T+c] + d*ln[T]+e*T^f Pressure,P[kPa] T[K]	
Min Temperature[C]	98.10
Max Temperature[C]	530.85
Coefficient Name	Antoine Coeff.
a	6.83402e+01
b	-1.10940e+04
c	0.00000e+01
d	-6.93279e+00
e	7.80947e+19
f	6.00000e+00

Table 6 – Additional Point Properties

Mass Vapour Enthalpy – Ideal Gas 20K H=a+b*T+c*T^2+d*T^3+…+ f*T^5 H[kJ/kg] T[K] g = Enthalpy Coeff [Defaul 1.0]	
Min Temperature[C]	270.00
Max Temperature[C]	5000.00
Coefficient Name	Ideal Coefficient
a	0.00000e+01
b	-2.11550e+01
c	2.49950e+03
d	-1.48420e+06
e	4.92180e+10
f	-6.95770e+14
g	1.00000e+00
h	0.00000e+01

Table 7 – Base Properties / Critical Properties

Molecular Weigth	122.17
Normal Boiling Pt[C]	284.00
Ideal Lig Density { kg/m3]	1048.53
Temperature [C]	530.86
Pressure[kPa]	4380.00
Volume[m3/kgmole]	0.37664
Acentricity	0.57944

Table 8 – Temperature dependent Properties

Property Package Molecular Props	
8PRSV-Kappa	0.00814
KD Group Parameter	0.00000
ZJ EOS Parameter	0.00000
GS/CS-Solubility Parameter	11.68752
GS/CS-MOL Vel[m3/kgmole]	0.10973
GS/CS-Acentricity	0.57944
UNIQUAC- R	6.82002
UNIQUAC-Q	5.71383
WilsonMOlar Volume [m3/kgmole]	0.10973
CN Solubility	11.68752
CN Molar Volume [m3/kgmole]	0.10973

Table 9- Additional Point Properties

Mass Vapour Enthalpy – Ideal Gas 20K H=a+b*T+c*T^2+d*T^3+…+ f*T^5 H[kJ/kg] T[K] g = Enthalpy Coeff [Defaul 1.0]	
Min Temperature[C]	-270.00
Max Temperature[C]	5000.00
Coefficient Name	Ideal Coefficient
a	0.00000e+01
b	-3.62671e+01
c	3.65767e+03
d	-2.33391e+06
e	8.69808e+10
f	-1.34240e+13

Table 10- Temperature Dependent properties

Thermodynamic and Physical Props	
Dipole Moment[Debye]	1.7875
Radius of Gyration[Angstrum]	4.16496
COSTALD[SRK]Acentricity	0.57944
COSTALD Volume[m3/kmole]	0.38183
Viscosity Coeff A	-0.54347
Viscosity Coeff B	-0.73403
Cavett Heat of Vap Coeff A	0.24527
Cavett Heat of Vap Coeff B	<empty>
Heat of Form[25C][kJ/kmole]	5.837e+004
Heat of Comb[25C][kJ/kmloe]	-4.022e+006
Enthalpy Basis Offset[kJ/kmole]	3.861e+004

4. Conclusions

Heterogeneous hydrogenation of nitro compounds using platinium nanoparticles as catalyst were investigated under continuous flow conditions are an important reaction in the chemical and pharmaceutical industries . In this study with the 2,4-dinitrotoluene model it was shown that hydrogenation kinetics in multicomponent mixtures can be described with rate equations based on single-compound experiments if the adsorption equilibria of 2,4-dinitrotoluene are included in the rate equations.Single-compound models are thus possibly applicable in the computer simulation of aromatic compounds.Similar experimental setup and computer calculation model by HYSYS software were suitable for 2,4-dinitrotoluene . The test reactor's continuous operation together with the standard periods at the beginning and the end of the experiments,enabled the effect of catalyst deactivation on the chemical kinetics to be eliminated.This is scarcely possible with batch reactor methods .Furthermore,since the effects of mass transfer and the reaction matrix(hydrogen solubility) on the observed rates were eliminated in the optimization of kinetic parameters,the obtained models are applicable to process computer simulators.

$$N_{GL}a_L = \frac{c_G - K_{GL}c_L}{\frac{K_{GL}}{K_L a_{GL}} + \frac{1}{K_G a_{GL}}} \quad [1]$$

$$D_{eff.} = D\varepsilon_p / \tau_p \quad [2]$$

$$\partial C/\partial t = D_{eff.}/\varepsilon_p r_p^2 [\partial^2 C/\partial\lambda^2 + (B-1)\,\partial C/\lambda\,.\partial\,\lambda] + r\rho_p/\varepsilon_p \quad [3]$$

$$B = A_p r_p / V_p \quad [4]$$

$$(\Delta T)_{max.} = \Sigma[C(-\Delta H_R)D_{eff.}] / k \quad [5]$$

$$\partial T/\partial r = k/\rho_p C_p r_p^2 [\partial^2 T/\partial\lambda^2 + \partial T/\lambda\partial\lambda] + \Sigma\, r(-\Delta H_R)/C_p \quad [6]$$

$$dn^G/dr = F_{in}^G - V_R N_{GL} a_{GL} - F_{out}^G \quad [7]$$

$$dn^L/dr = F_{in}^L + V_R N_{GL} a_{GL} + V_R N_{LS} a_{LS} - F_{out}^L \quad [8]$$

Corresponding author:
Mohammad Reza Saboktakin,
International Research Institute of Arian Chemie Gostar, Tabriz, Iran,
Tel/Fax: +00984116694803
Email: saboktakin123@yahoo.com

5. References

1) Nishimura, S., 2001, "Handbook of heterogeneous catalytic hydrogenation for organic synthesis", *Wiely-Interscience*.
2) Kabalka, G.W.; Vama, R.S., 1991, " Comprehensive organic synthesis"; *Eds.*

Trost. Fleming, I, pergamon Press, Oxford, 8, pp363.

3) Rylander, P., 1979, "Catalytic hydrogenation in organic synthesis"; *Academic press, New York*.
4) Tundo, P., 1991, "Continuous flow methods in organic synthesis"; *Ellis Harwood, New York*.
5) Ehrfeld, W.; Hessel, V.; Lowe, H., 2000, "microreactors: New technology for modern chemistry"; *Wiley-VCH, Weinheim*.
6) Zhang, L.; Rana, T., 2004, "For a recent solid-phase method for the synthesis of DHPM C5 amindes"; *J. Comb. Chem*., 6, pp457.
7) Tri, T. M.; Massadier, P.; Gallezot, P.; Imelik, B., 1982, "Metal-support and metal additives effects in catalysis", 11, pp141.
8) Moreau, C.; Geneste, P., 1990, "Theoretical aspects of heterogeneous catalysis"; *Van Nostrand Reinhold, New York*, 8, pp256.
9) West, A.R., 1998, "Solid state chemistry and its applications"; *John Wiley and sons Ltd.; Chichester,England*.
10) Klug, H.P.; Alexander, L.E., 1954, "X-ray diffraction procedures for polycrystalline and amorphous materials", *wiley, New York* .
11) Fukai, Y., 1993, "The metal-hydrogen system, in Materials science, 21, pp142.
12) Winter, C.J.; Nitsch, J., 1988, "Hydrogen as an energy carrier", 5, pp136.
13) Cox, K.E.; Thompson, A.W.; Bernstein, I.M., 1976, "Effect of hydrogen on behavior of materials, *The metallurgical society of AIME, New York*, 3, pp245.
14) Allen, L.; Suchanek, A., 1998, "Consider the Options for Meeting Stringent European Gasoline Specifications", *Hart's Fuel Technol. Manage.* **8**(2), pp14.

4/1/2010